Manufacturing Review

REVIEW ARTICLE

OPEN 🔓 ACCESS

Vapour deposition technologies for the fabrication of hot-forming tools: a review

Gonzalo G. Fuentes[1,*], Eluxka Almandoz[1], Rafael J. Rodríguez[1,5], Hanshan Dong[2], Yi Qin[3], Sonia Mato[4], and Francisco Javier Pérez-Trujillo[4]

[1] Center of Advanced Surface Engineering, AIN, Cordovilla-Pamplona E31191, Spain
[2] School of Metallurgy and Materials, University of Birmingham, Edgbaston B15 2TT, UK
[3] Dept. of Design, Manufacture and Engineering Management, The University of Strathclyde, G1 1XJ Glasgow, UK
[4] Dpto. de Ingeniería de Superficies, Universidad Complutense de Madrid, 28040 Madrid, Spain
[5] IMEM Department, Universidad Pública de Navarra, E31006 Pamplona, Spain

Abstract – This paper reports recent developments of vacuum coatings technologies for hot-forming tooling applications. Whilst well implanted in the machining and cutting industry, vacuum coatings face important challenges for the fabrication of forming tools, and more specifically in hot forming, due to the extreme operation conditions to be met, such as high loading forces, impact/thermal cycling, working material adhesion, etc. Present and future coatings adapted to hot work tooling are discussed in this paper: transition metal nitrides, carbon nitrides, borides and mixed oxides are among the currently postulated coating formulations for high temperature forming. The study is complemented with current strategies of characterizing the properties of the coatings in the adequate environment of high temperatures and contact loadings. To this aspect, a number of examples, from using standard laboratory equipment to the use of in-house developed tribological set-ups, are given, together with recent findings obtained from the authors' research groups. The data available is, however, quite limited from the scientific literatures on the field trials with reliable, statistical relevance, which is, probably, attributed to the high costs normally incurred for carrying out experiments in real industrial environment. Nevertheless, we could still draw a conclusion of that vacuum coating for tooling applications is at a front edge of knowledge generation and technology transfer to industry, and while being already mature, there is still a needed effort for significant industrial up-take from the novel coatings developed or being under the development.

Key words: Hot forming, Physical vapour deposition, Chemical vapour deposition, Tools/Moulds, Tool failures, Tool life

1. Introduction

Hot forming encompasses a series of manufacturing processes where high temperature working material in the solid or molten state is reshaped until a given final designed geometry is achieved. Hot forming is ubiquitously present in all areas of the manufacturing industry, from the automotive, aeronautics, construction, energy, metal-prosthetic and several others. The advantages of hot forming over other manufacturing processes are related to the ability of the materials to increase its workability when the temperature is raised. Therefore, hot forming is commonly utilised when materials are difficult to form at room temperature, due to poor intrinsic workflow (e.g. Inconel, Ti-alloys), or when difficult large size geometries of high strength materials need to be attained. Another important driving force to hot forming is the processing speed. As in other forming processes, hot forming can be designed for mass production if appropriate automatization and handling systems compatible with high temperature working materials are implemented. The solidus-liquidus phase diagram line of the working material determines the type forming process. Below the liquidus line, the working material remains in solid state. In this case, the forming requires a press and a shaping mould. Above the liquidus line, the molten metal (or polymer) can be injected at high pressure inside a die (casting) or it can be flown simply by the effect of gravity or alternatively a centrifugal force. Near the liquidus line, solid-liquid state coexists, giving raise to specific tixoforming processes.

*e-mail: gfuentes@ain.es

The mould/die constitutes an essential component of hot forming, as they are the first interacting interface with the working material. It is the press force-transmitting element when the metal is below its liquidus line and the receiving element when the material is in a molten or solid-liquid state.

Hot work material interacts with the mould surface at elevated temperatures and large contact pressures. In addition, mass manufacturing demands continuous operations where the tool surface is held to thermal cycles of annealing and cooling over large periods of serial manufacturing. For example, typical series production of Al-die casted parts can exceed 100 to 500 thousand units. All these cause tool surfaces to degrade by the effect of thermal fatigue, abrasion and work material soldering (galling) at most. Tool surface degradation is in fact one of the major causes of productivity losses in the manufacturing industry; considering all varieties of manufacturing, it is estimated that in Germany alone, the consumption of oil-derived lubricants for wear prevention in tooling and gear element represents up to $1–2 billion/year [1] for manufacturing industries. In US only, it is estimated that wear and friction derived losses exceeds $100 billion per annum [2].

Vacuum coatings based on vapour phase deposition are gaining importance as forming tool surface protection technologies. Physical Vapour Deposition (PVD) and Chemical Vapour Deposition (CVD) are well consolidated technologies for the tooling sector. These techniques provide coatings (thin films 1–5 microns thick) of outstanding hardness (>2500 HV), toughness and wear/thermal resistance, making its use essential for nearly all value added cutting tools. Surface Engineering is multidisciplinary knowledge area and a consolidated enabling technology for the tooling sector in Europe and worldwide. In Europe alone, the surface engineering segment represents c.a. 12 billion €, and employs around 500,000 staff, including themochemical and galvanic based treatments.

Vapour deposited coatings have found their maximal performance for cutting tools [2–5] due to the specific contact and interfacial interaction between tool and working material; i.e. normal versus shear forces, sliding speed, low impact, tool cooling regime and mechanical properties of the base (tool) material. However, PVD or CVD coatings are only partially present in forming applications, and their full potential is still unrealized. Forming operations require extremely high contact forces (normal and shear) between tool and work material, low sliding speed in comparison to these required in cutting. Hot forming or die casting tools are held to intensive thermal cycles of hundreds of degrees of amplitude. In addition, die surfaces are exposed to high temperatures and therefore to oxidation and thermal decomposition. Finally, the mechanical properties of forming tool materials are not as large as these utilized as cutting tools; as a consequence, the survival of hard coatings is limited due to insufficient loading support problems. All these process characteristics make the vacuum coatings to find more difficulties to outperform on forming tools.

Significant progresses have been reached in the search for novel vacuum coating formulations to perform in hot working applications. In this context, this review intends to give a concise overview of the state of the developments in PVD and CVD technologies for hot forming. The review is targeted to provide basic and relevant information to mechanical engineers of this field of the manufacturing, and not on advanced and detailed scientific findings; as there are excellent review articles covering these issues, some of which are cited here. The review is organised as follows: first, a summary over the basic properties of benchmark PVD and CVD coating for high temperature applications will be given; second, the mechanical and tribological properties of thin films in laboratory stations adapted for high temperature conditions will be discussed. Various field trials reported in the literature as well as some non-published results from our research group will be presented, ending up with some currently observed research trends. The review includes references to scientific literature where coating fundamentals, laboratory tests and field trials are jointly reported.

2. Coatings and vacuum deposition technologies

2.1. Coating materials

Transition metal nitrides have been considered as the flagship coating materials for tooling applications. Titanium nitride (TiN) [6] is the most extendedly used coating for cutting and forming tools due to its high hardness, low-medium coefficient of friction (COF) and toughness. Titanium carbon nitride (TiCN) shows a higher hardness and lower COF than TiN [7, 8], but reduced thermal stability. In fact, this coating requires coolants, especially during high speed machining operations, to avoid its premature oxidation by overheating. Aluminium titanium nitride (AlTiN) coatings [5, 6, 9] were implemented for cutting tools in the 1990s and are used widely at the present time for high speed and dry-machining inserts due to their high hardness (greater than that of TiN) and elevated thermal stability. Chromium nitride (CrN) [2, 10, 11] shows inferior hardness to that of TiN but low adhesive COF, permitting its application in plastic injection moulding and other forming operations where galling needs to be attenuated. This is due to the low tendency of CrN to stick to the working material during processes requiring high contact stresses at the tool/material interface. At present, recently developed CrCN [12] coatings are found to exhibit even lower adhesive COF to those of CrN when sliding on stainless steels. AlCrN [2, 13] coatings have only reached the market in the last decade. These coating formulations posses a high hardness and toughness and an outstanding oxidation resistance, due to its ability to form a protective chromium oxide overlayer. Finally, the family of solid lubricious coatings, such as diamond like carbon (DLCs), WC-C [2, 14] or MoS_2 [15] is utilized on bearing parts and plastic injection mould inserts. Nevertheless the application of carbonaceous films is restricted to applications where the working temperatures do not exceed 300–350 °C. Table 1 gathers some engineering relevant macroscopic magnitudes of some TM nitride and Al_2O_3 coatings frequently used in hot forming applications [16, and Refs. therein].

The family of the ternary TiAlN [17–19], TiSiN [20], CrAlN [21, 22] and CrSiN [23] and quaternary transition metal nitride coatings, especially TiAlSiN [24–26] and

Table 1. Structure, mechanical and thermal properties of some hard coating materials (Ref. [16] and references therein).

Material	Hardness (kg mm^{-2})	Young's modulus (kN mm^{-2})	Thermal expansion coefficient (μm/m K^{-1})	Thermal conductivity (W/mK)	Melting point or decomposition temperature (°C)
TiN	2000 < 3680	440	9.35	20–28	2949
TiB$_2$	3370	480	8.0	25	2900
VN	1500	460	8.1	11.3	2177
ZrN	1500	510	7.2	20.5	2982
CrN	1100	400	2.3–3.5	10.8	1500
Cr3C2	1300	400	10.3	n.a.	1810
Al$_2$O$_3$	4000	400	9.0	25–30	2300

CrAlSiN [27, 28] thin films are attracting significant attention in surface engineering for hot working applications. The interest on these coatings strives in their resistance against wear and oxidation at high temperatures, which is of great importance for the surface protection of high speed machining or hot forming tooling parts.

2.2. Coating design strategies

PVD and CVD permit the design of a variety of film architectures with the aim to outperform the protective characteristics of single-layer configurations. Figures 1a–c show different multilayer structures developed using the cathodic arc PVD technique; (a) a gradient CrCN coating [12], (b) a nitride/nitride nanomultilayered TiN/CrN arc evaporated film (c) and a nitride/oxide multilayered CrAlN/CrAlO arc evaporated coating. Gradient composition films containing a hard layer at the interface and a low COF outer layer is a well-developed solution for several applications in the manufacturing sector [13, 29]. Another common strategy to enhance the mechanical performance of PVD films is the design of load-adaptive layers, or layers which respond upon an external environment, such as high friction or heat [29, 30].

Nano-multilayered coatings made of two different compounds (usually hard ceramic-ceramic or metal-ceramic) are found to exhibit the highest hardness/toughness when the nominal bi-layer thickness ranges between 5 and 15 nm [2, 30, 31]. Stueber et al. [31] classified nano multilayered structures into two major categories: (1) multilayer coatings without epitaxial stabilization and (2) multilayer coatings with epitaxial stabilization; where epitaxial stabilization is related to the ability of one single constituent to develop local crystalline metastable structures thanks to the template effect of the other single constituent.

The deposition of immiscible phases in the form of thin film can lead to the formation of finely grained coatings (denoted as *nano-composites*). This variety of coatings shows superior values of hardness and toughness than these of their single constituents. It is commonly found that the incorporation of silicon in TiN [20, 32, 33], or AlTiN films [25, 26, 34], in quantities of around 8–10 at.%, increase their hardness values by a factor of 1.5–2. In addition, (Al, Si)TiN nano-composites retain their mechanical properties even after annealing temperatures of above 800–900 °C [20, 25, 26].

2.3. Coating technologies

Cathodic Arc Evaporation (CAE), Magnetron Sputtering (MS) and to a lesser extent Electron Beam (EB) constitute at present the core group of PVD techniques for industrial tooling protection. In fact, there exists a great variety of PVD techniques, but this group alone share more than 95% of the PVD market, in terms of both equipment sales and services. With regards to Chemical vapour deposition, depending on the temperature and the presence or absence of plasma assisting processes, it can be classified into thermal CVD and plasma activated or plasma enhanced CVD (PACVD or PECVD respectively).

Cathodic Arc Evaporation (CAE) sources are probably the most widely utilized technique for industrial tooling protection. In CAE, a high electron current density is discharged onto a target material, producing a fast evaporation rate at its surface. The energy dissipated during the process sprays the evaporated atoms towards the substrate at energies of tens to some hundreds of eV. This feature, and the high ionization produced during the electron discharge (up to 90% of the evaporated species), produce uniform and dense films, with compressive residual stresses. The deposition of metal compound films can be obtained by introducing reactive gases such as N$_2$, O$_2$ or C$_2$H$_2$ during the discharge process.

Part of the energy dissipated on the target surface during CAE is able to produce micro-sized particles (*micro-droplets*) that can also be sprayed towards the substrate. In general, these micro-droplets are barely detrimental for conventional machining tools provided the net-shape of cutting edges remains unchanged upon deposition. The presence of these micro-particles, however, can be detrimental for forming tools. In these cases, a surface repolishing process needs to be performed after a PVD CAE treatment. To avoid an excessive deposition of micro-particles, different arc sources design strategies are in use, such as the Lateral Arc Rotating Cathode (LARC) configuration, or the filtered arc.

Magnetron sputtering sources are based on the confinement of low pressure plasmas around an evaporation target by an appropriate configuration of static or alternating electric field (DC, DC-pulsed, AC) superimposed to a static permanent magnetic field. Ions from the confined plasma bombard the target material, producing the sputtering of atoms from the target towards the substrate. The energy of the sputtered atoms is usually not greater than a few eVs, and their ionization rate
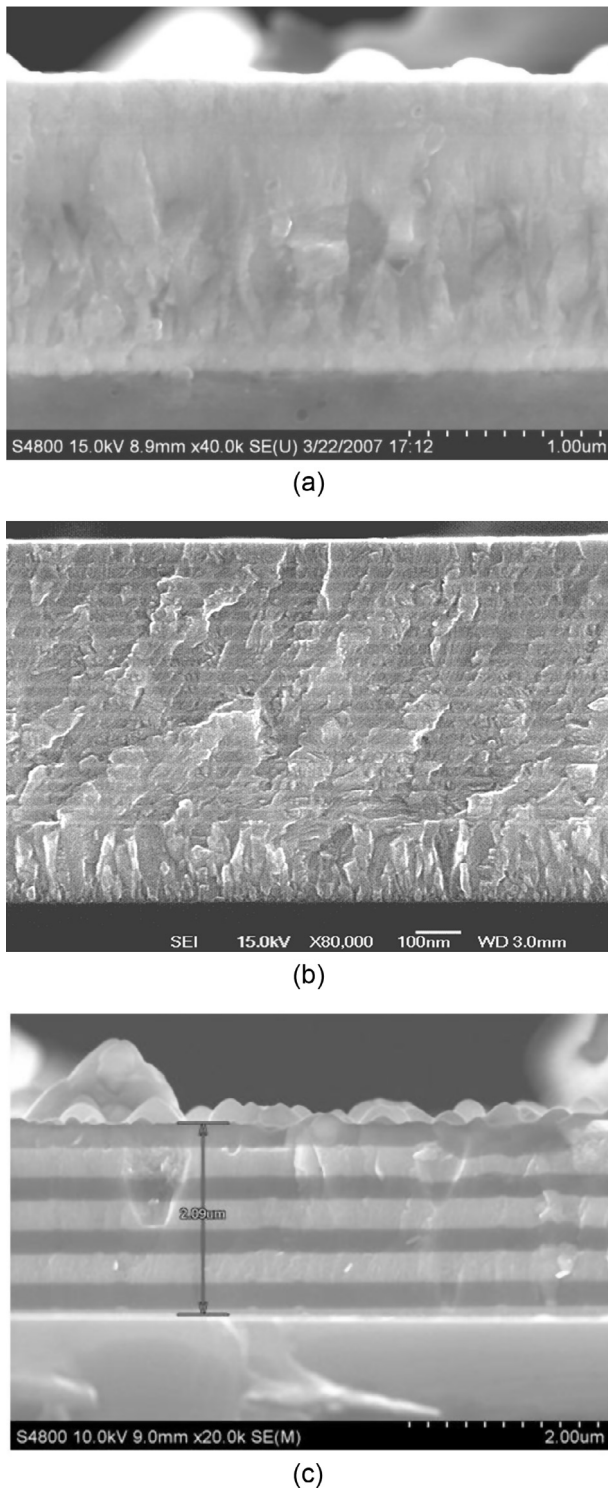
(a)

(b)

(c)

Figure 1. Different multilayer structures developed using the cathodic arc PVD technique; (a) a gradient CrCN coating [12], (b) a nanomultilayered TiN/CrN and (c) a CrAlO/CrAlN multilayer.

accomplished polarizing the substrate with a negative potential (bias potential) of some tens or few hundreds of volts. Under these conditions, the deposition of sputtered atoms is produced simultaneously to the bombardment of ionized inert species (typically Ar^+ ions) onto the growing film. This combined process, so-called Ion Beam Assisted Deposition (IBAD), provides sufficient energy per arriving atom to form dense and well-adhered films. The ionization and energy of the sputtered atoms can also be strongly increased using high power impulse magnetron sources (HIPIMS) [35]. HIPIMS utilizes high energetic electromagnetic mega-watts/cm^2 millisecond pulses during the sputtering process to achieve ionization rates of almost 100% of the depositing species.

Thermal CVD requires high temperatures in the range 800 °C and 1000 °C, hence limiting the type of materials suitable to be treated by this technique due to thermal-degradation effects. In fact, the high temperatures reached during CVD cycles often produce size distortions of the tools. Thermal CVD films exhibit very high adhesion strength, due to temperature-induced atomic diffusion at the coating/substrate interfaces. This fact converts thermal CVD into a recommended technique to be applied to tools subjected to strong normal and shear forces (cold/hot forging, metal forming). The most commonly utilized coating materials for tooling protection are titanium nitride (TiN), titanium carbon nitride (TiCN) and chromium nitride (CrN). Other transition metal carbon nitrides such as hafnium or vanadium can be deposited by CVD, showing a good combination of hardness and low COF.

Alternative to thermal CVD driven processes is the plasma activation of the precursor gases using configurations such as hot-filaments, hollow cathodes or microwave sources. This activation can promote the formation of high quality thin films even at deposition temperatures as low as 200–300 °C. These processes are named plasma activated CVD (PACVD), and represent a feasible alternative to deposit films onto a larger variety of substrate materials, specifically hot work steels.

2.4. Vacuum coatings in hot forming

One of the difficulties of hard coatings on forming tools is the hardness and elastic modulus mismatch between coating and tool surface. Hot forming tools are based on hot work ferritic steels containing Cr, Mo and other alloying elements which provide resistance to oxidation e.g. Cr-steels H10-H19, W-steels H20-26 or Mo-steel H46. The hardness required for hot work steels (45–55 HRC) is not as large as for cold work or machining applications (>60 HRC). This is due to fact that, on the one hand, high fracture toughness is required; therefore high hardnesses are not recommended. On the other hand, operational temperatures restrict the tempering state of the steel.

As a consequence of this mechanical mismatch, the tool steel need to be surface hardened to create a load support layer (30–100 microns thick) able to prevent the early failure of the coating due to fracture by stress accumulation (the so call *thin ice layer effect*). Thermochemical treatments, nitriding and carbonitriding, by molten salts, reactive gas or plasma nitriding (PN) can be applied to this purpose. The combination of a thin
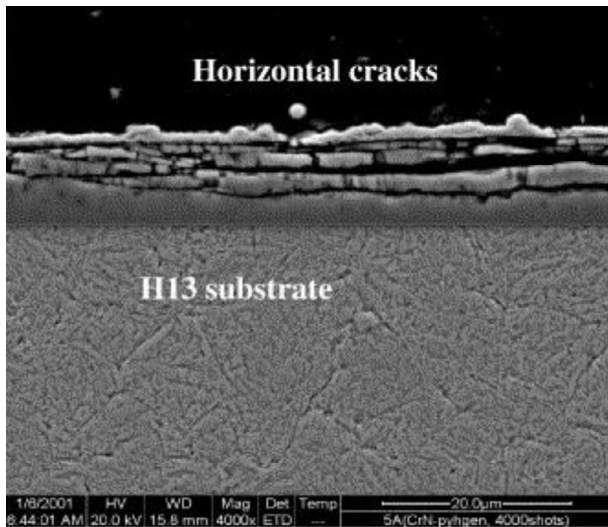
is generally poor (below 10% of the total sputtered atoms). Both, low ionization and energy makes necessary the post-ionization and acceleration of the sputtered species to achieve sufficient impact energy during the deposition. This can be

Figure 2. Horizontal cracks in CAE-graded CrN coating on un-nitrided H13 tool steel after 12,000 Al-cast shots (from Figure 11 of [39]).

film and a thermochemical treatment is denoted as Duplex treatment [36–38].

Thermal fatigue is another important surface effect detrimental for hot working tools. It is influenced by a combination of coating-substrate mechanical and thermal expansion response mismatch. Substrate expansion/shrinking due to thermal annealing cycles induced stress in the coatings that release in form of cracks. Crack initiation may lead to a fracture propagation towards the tool steel or can induce chemical reactions between the working material and the die; e.g. as in Al die casting [39], where Al reacts with the steel elements forming brittle Fe-Al-Si ternary intermetallics. This chemical interaction between working material and tool surface constitutes an undesired effect for hot work tools. Figure 2 shows as an example the severely cracked microstructure of a CrN coated H13 hot work steel after 12,000 Al-casting shots [39]. Persson et al. [40] reported that, generally speaking, surface treatments decreased the resistance against surface cracking of the tool steels. Galling is the adhesion/soldering of working material onto the tool surface causing its severe wear. It becomes another relevant performance parameter in hot forming.

Finally, vacuum coatings should be as conformal as possible, that is to say, they should keep homogeneity through the mould surface. This is often complex to achieve since mould surfaces contain deep cavities, holes and trenches, which may jeopardize the deposition of homogeneous thickness distributions or even produce blind zones, were the vapour flux is not able to reach. In order to solve this problem, various strategies such as the sample stage planetary rotation or the application of negative polarizations (Bias) can be attempted. The homogeneity of ion bombardment on biased components also depends on the presence of holes and trenches, due to the energy losses of the impinging ions when crossing plasma sheath regions. A precise control over the electron densities in glow-discharges, the working pressure or the bias potential can minimize the energy losses of the bombarding ions, and

hence enhance the film microstructural homogeneity on complex surface geometries [41].

3. Structural, mechanical and tribological properties of thin films

3.1. Microstructural properties of PVD and CVD coatings

Transition metal nitride (TM-N) thin films (i.e. groups **4**: *Ti, Zr, Hf*; **5**: *V, Nb, Ta*; and **6**: *Cr, Mo* and *W*) form crystalline structures of the group B1-NaCl, i.e. a face centred cubic lattice with a high atomic density (i.e. typically larger than that of the pure metals and their oxides). TM-Ns have an outstanding mechanical and structural strength due to a mixture of ionic and covalent atomic bonding [42]. They have high thermal and electrical conductivities, high IR reflectivity, and high absorption in the VIS-UV [43]. When deposited in the form of thin films, TM-Ns develop a polycrystalline dense-column microstructure, which can be tailored by changing the deposition parameters, with the aim to optimize their mechanical properties. For tooling applications, the microstructure is designed to exhibit strengthening mechanisms to difficult the displacement of dislocations and hence the film deformation or cracking. Deposition parameters such as the temperature, the pressure or the averaged bombardment-energy per substrate-arriving atom determine the coating microstructure. A comprehensive review on microstructural design of thin films can be found in reference [44].

Al and Si are typical alloying elements for TM-Ns coatings for hot working tools (e.g. TiN and CrN mainly). Al replaces the TM in the cubic lattice structure, diminishing the interatomic spacing, giving rise to higher hardness and toughness. In addition, at high temperatures Al can form Al_2O_3 surface compounds resulting in effective barriers against thermal oxidation and self lubricated top coats [4–6]. Mayrhofer et al. [45, 46] explained the basic mechanism behind the high hardness and high thermal stability of these coatings, and how they form hardened solid solutions or multiphase components in TiN, CrN or ZrN systems. In TiN for example, for an AlN mole fraction x below 0.7, the $(Ti_{1-x}Al_x)N$ coatings crystallize in a supersaturated cubic NaCl-type structure where Al substitutes for Ti. The metastable cubic $(Ti_{1-x}Al_x)N$ structure decomposes during annealing forming extremely fine-scale precipitates of cubic TiN and cubic AlN domains, before phase transforming into the thermodynamically stable constituents (i.e. cubic NaCl-type TiN and ZnS-Wurtzite-type AlN). The formation of the cubic TiN and AlN, with crystallographic coherent interfaces within the cubic $(Ti_{1-x}Al_x)N$, matrix results in a hardness enhancement by providing additional obstacles for the dislocation movement.

Silicon has also been incorporated in TiN, CrN, AlTiN and AlCrN at concentrations between 2 and 8 at.%, which lead to ternary and quaternary coating stoichiometries. More specifically, the quaternary coatings of the family TiAlSiN and CrAlSiN have received particular attention in hot work applications and cutting, due to their outstanding mechanical and thermal stability. These coatings consist of solid solutions

(Cr/Ti, Al, Si)N, where Al and Si replace Cr/Ti atoms in a metastable B1-NaCl crystal structure. The addition of Si in the cited quantities induces a significant grain refinement and a dense film microstructure more resistant to oxidation and contact fatigue. These films can also develop other crystalline structures such as h-AlN or amorphous SiN depending on their stoichiometries and thermal stabilities [25–28].

With regards to TiAlSiN films, Kim et al. [25] reported hardnesses of up to 46 GPa for coatings deposited between 300 and 350 °C, and with Si contents between 2.8 at.% and 3 at.%. They attributed these high hardnesses to the formation of highly crystalline TiN. Flink et al. [26] showed that $(Ti_{0.33}Al_{0.67})_{1-x}Si_xN$ CAE films were X-ray amorphous wurzite based compounds for Si contents higher than $x > 17$ at.%, whereas for $4\% < x < 17\%$, the films consisted of solid solutions (Ti, Al, Si)N exhibiting high hardness and cutting performance.

The mechanical properties of the CrAlSiN films are determined, as in the case of the TAlSiN, by the stoichiometry and the microstructure. Hardness values of up to 40 GPa have been reported by Ding et al. [47] for CrAlSiN coatings, as deposited by lateral arc rotating cathodes, with (Al + Si)/Cr concentration factors of 1.62. For greater atomic concentrations of Aluminium the hardness drops significantly. Rafaja et al. [28] determined for CrAlSiN CAE deposited films that stoichiometry factors Cr/(Cr + Al + Si) < 0.52, developed hexagonal AlN crystalline phases. Endrino et al. [27] showed that the addition of Si has a grain refining effect in the CrAlN structure. Zhang et al. [48] have investigated multilayered CrAlSiN films deposited by CAE. The film exhibited a superlattice structure of B1-NaCl of (Cr, Al)N layers alternated with h-(Al, Si)N with a bilayer period λ of 7 nm and a hardness of 52 GPa.

The thermal stability and the oxidation resistance of the TiAlSiN and CrAlSiN systems have been extensively investigated over the last years [25–28]. In general terms it has been found that the CrAlSiN system exhibits greater oxidation resistance than TiAlSiN. It is commonly accepted that the formation of aluminium and silicon oxides at the surface of the coatings generally reduce the oxidation kinetics by oxygen barrier effects. Chang et al. [49] found than Al and Si inhibited the formation of Cr_2N and the coarsening of CrN grains during air oxidation of CrAlSiN at 800 °C. Won et al. [50] claimed that the good oxidation resistance of the CrAlSiN films is attributed to the formation of oxide crystallites of Cr_2O_3, α-Al_2O_3 and amorphous SiO_2 through outward diffusion mechanisms of Cr, Al and Si species. Flink et al. [26] also studied the thermal stability of the different TiAlSiN coatings and reported on spinnodal decompositions between 600 °C and 1000 °C into c-TiN, c-AlN, h-AlN phases depending on the original film compositions. The thermal conductivities of the TiAlSiN and CrAlSiN coatings have also been estimated by Martan and Benes [51].

The oxidation behaviour of CrAlSiN arc evaporated PVD coatings deposited on structural steels in 100% water vapour stream at 650 °C have been also investigated by our group. The coatings were exposed to cyclic annealing-cooling steps. Figure 3 shows the SEM cross sections pictures of the CrAlSiN coatings respectively after 0, 500 and 1000 h of annealing treatment as labelled. The elemental analysis recorded on the 1000 h treated coating by glow discharge optical emission spectroscopy (GDOES) is also shown. After the 1000 h treatment, the oxide overlayer grown on the CrAlSiN coating is barely visible by SEM, reflecting the resistance of these materials to oxidation. A finer analysis by GDOES indicated that the oxide layer formed on the CrAlSiN coating after the annealing treatment is around 0.3–0.4 microns with the maximum concentration of oxygen at 0.1 microns in-depth.

3.2. Tribological properties of PVD and CVD coatings at high temperature lab tests

Several metal forming processes such as high pressure Al-injection casting, or hot extrusion are carried out at temperatures between 200 °C and 800 °C. Therefore, the understanding of the tribological response of PVD and CVD hard coatings at these temperatures is of high technological importance to improve the performance of hot forming tooling elements. The temperature affects the coefficient of friction of coating materials and their wear properties. Oxidation rate, structural relaxation and thermal contact determine the tribological properties of coating/substrate systems. The tribological properties of TM-Ns have been exhaustively investigated, and in fact, various reviews on tribology of coatings can be found in the scientific and technical literature (see e.g. [2]).

The coefficient of friction is one of the most relevant parameters in forming tool workpiece processing. Various observed COF trends are reported. For example, the COF of TiN arc plated coatings against SiC have been found to increase as the testing temperature increases from 200 °C to 600 °C [52]. Contrarily, Kutschej et al. [53] reported that the COFs of $Ti_{1-x}Al_xN$, and $Ti_{1-x}Al_xN$ doped with Hf, Nb and B coatings [54], deposited by DC magnetron sputtering, decreased as the temperature increased from RT, 500 °C and 700 °C. This can be seen in Figure 4.

Jianxin and Aihua [52] reported a similar behaviour for $Ti_{35}Al_{65}N$ coatings tested up to 600 °C, attributed to the formation of an Al_2O_3 top layer. Walker et al. [55] found that the COF of CrAlYN/CrN multilayered PVD coatings decreased when the temperature of the tests increased from RT to 300 °C and further to 600 °C. The formation of a "glaze" layer from oxide based particles (aluminium and chromium based) at 600 °C was responsible for the low COF and wear rates of the CrAlYN/CrN multilayered coating.

Hovsepian et al. [56] studied the tribological response of TiAlCrN/TiAlYN and TiAlN/VN superlattice at RT and 850–950 °C, also exhibiting a reduction of the COF at high temperatures. They found two different re-adaptation mechanisms for each of the tested films. For TiAlCrN/TiAlYN, the Y migrated to the grain-column boundaries, whereas TiAlN/VN forms highly lubricious vanadium-oxides due to high flash temperatures at the asperity contacts on the surface.

Polcar et al. [57, 58] found that the COF of CrAlN, CrAlSiN and AlCrSiN coatings showed different response upon the testing temperatures. The counterpart utilized also influenced the temperature evolutions of the COFs. For example for AlCrSiN, the COF decreased linearly with the temperature when a 440 °C steel ball was used. In contrast, the COF increased upon the test temperature when an Al_2O_3 ball was
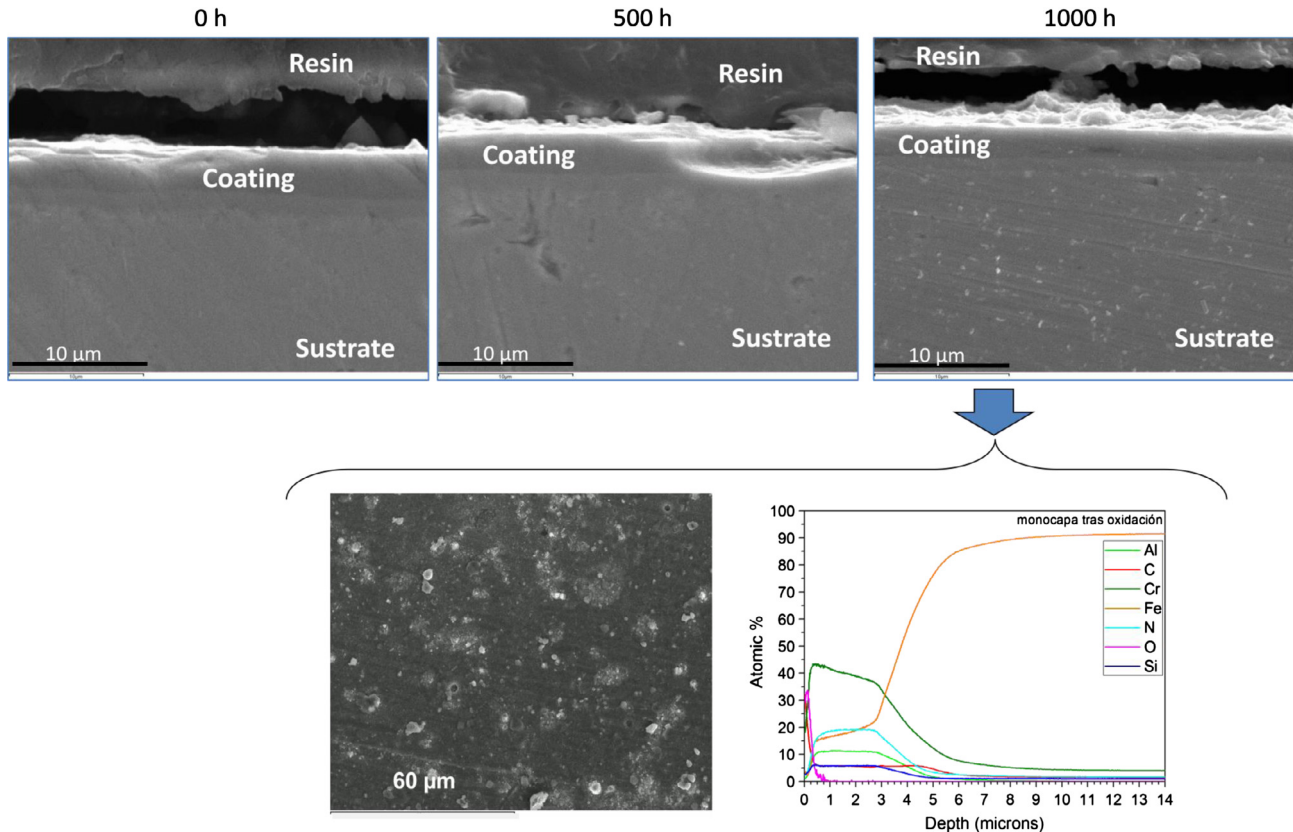
Figure 3. SEM cross sections pictures of CrAlSiN coatings after 0, 500 and 1000 h of annealing treatment at 650 °C in the presence of a 100% water vapour. Bottom: top view of the CrAlSiN film after 1000 h and the corresponding GDOES chemical in-depth profile.
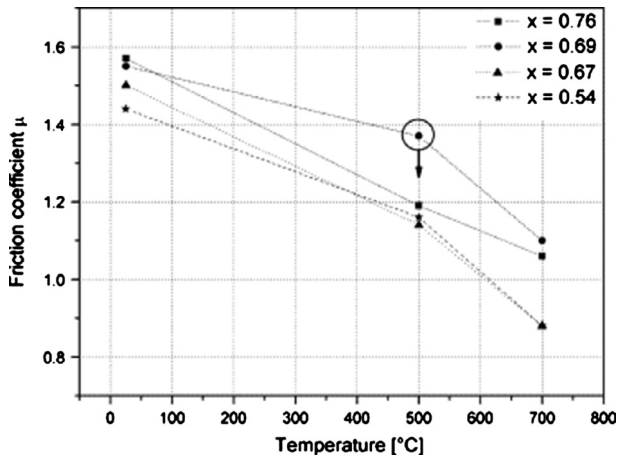

Figure 4. Average friction coefficients of $Ti_{1-x}Al_xN$ coatings with different Al contents depending on the temperature against stainless steel balls (from Figure 7 of [53]).

type Magnéli-phases V_2O_5 with weakly bonded lattice planes and low melting temperature, which result in effective low COF values. Silver demonstrates relatively low shear strength, and can reduce the friction coefficient on hard surfaces during sliding wear [60]. Different authors have investigated the role of V in VN [62], TiAlN [62, 63] and CrAlN [62, 64] coatings. The authors reported the optimal working temperature for V doped hard coatings to be in the range 600–700 °C with concentrations between 0 and 30 at.%. These adaptive coatings have been developed for extreme and durable condition, i.e. aerospace, gears and bearings in transport. Surface textured TiAlCN coatings containing MoS_2 and Ag exhibited a good response to high temperature friction at 600 °C due to the migration of Ag and formation of silver molybdate [65] and tantalates [66] phases onto the surfaces.

Wear resistance is another relevant coating macroscopic property influenced by the temperature. It is a common finding that, whereas the temperature diminishes the COF of several coating-counterpart systems, the wear rate increases as the temperature increases. This occurs mainly because the temperature (1) diminishes the hardness of vapour deposited coatings due to the recovery of structural lattice defects, and (2) produces oxidation of the film surfaces. Kutschej et al. reported [54] these on $Ti_{1-x}Al_xN$ magnetron sputtering coatings with an Al/Ti ratio of 2 and 5 at.% of X (X = Hf, Nb, B) at 25, 500 and 700 °C, as it is shown in Figure 5. In addition, $Ti_{1-x}Al_xN$ PVD coatings exhibited different wear rates
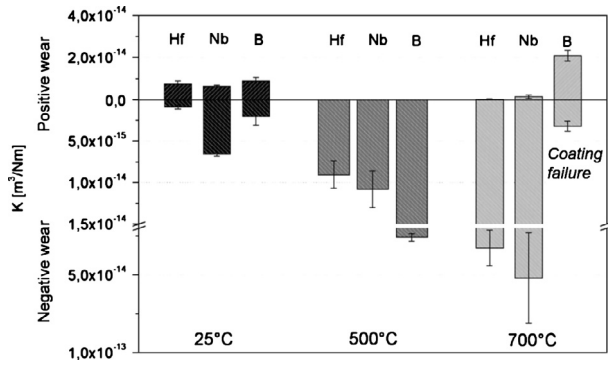
tested, reflecting the important influence of the counterpart in the test evaluation.

Vanadium and Silver have been introduced as alloying lubricious elements in vacuum coatings to enhance their tribological performance [59–66]. The lubricating effect of Vanadium is based on the formation of vanadium oxides of the

Figure 5. Positive and negative wear rates of Ti-Al-X-N coatings with an Al/Ti x_T = 2, and a 5 at.% of X (where X = Hf, Nb, B) at 25, 500 and 700 °C as labelled (from Figure 5 of [54]).

responses upon testing temperature depending on their Al content. For Al contents below 50 at.%, the wear rate at 700 °C was greater than that measured at RT. For Al concentrations above 65 at.% the temperature response exhibited the opposite trend, so that at 700 °C the wear rate measured was smaller than that at RT [54]. Equivalent tribological responses were reported on TiN, $Ti_{55}Al_{45}N$ and $Ti_{35}Al_{65}N$ PVD coatings, i.e. the wear rate increased as the testing temperature increased when the Al concentration of the films is smaller than 65 at.%, as for the TiN and $Ti_{55}Al_{45}N$ and decreased for the coating $Ti_{35}Al_{65}N$, where the Al concentration reached a 65 at.% [52] (see Figure 6). Hardell and Prakash [67] reported that the wear rates of commercial TiAlN arc deposited coatings on tool steels exhibited similar values at RT and at 400 °C.

CrN and Cr/CrN multilayered arc evaporated coatings exhibited a good thermal stability at temperature ranges between 600 and 800 °C [11]. The coatings retained good wear rate values around $1–10 \times 10^{-6}$ mm^3/Nm, though larger than typical wear rates measured at RT for arc evaporated CrN films [10]. Sánchez-López et al. [68] reported slight increments of the wear rates from RT to 650 °C for magnetron sputtering CrAlN and CrAlN films doped with Y or Zr. In another study [58] the wear rate of CrAlN, CrAlSiN and AlCrSiN PVD coatings against alumina increased as the temperature of the tests increased from RT to 500 °C. More specifically, whereas the tribological properties and adhesion strength of these coatings were evaluated as highly performing at RT, the tests at high temperature revealed a relatively poor wear resistance at temperatures above 400 °C. The authors actually did not find any clear explanation on this observation.

Alternatively Faga et al. [24] observed that the wear rates of the AlTiSiN nanocomposite coatings decreased when the tribological tests were carried out in a ball-on-disc configuration at 600 °C using a polycrystalline alumina balls with respect to those measured at RT. Fuentes et al. [34] confirmed that TiAlSiN films, with stoichiometries $Ti_{0.31}Al_{0.1}Si_{0.06}N_{0.53}$ and $Ti_{0.23}Al_{0.12}Si_{0.09}N_{0.55}$, developed a oxide based protective tribofilm at the sliding contact interface at 200 °C, 400 °C and 600 °C, able to provide additional wear protection properties to the film/substrate system. This is better reflected in Figure 7
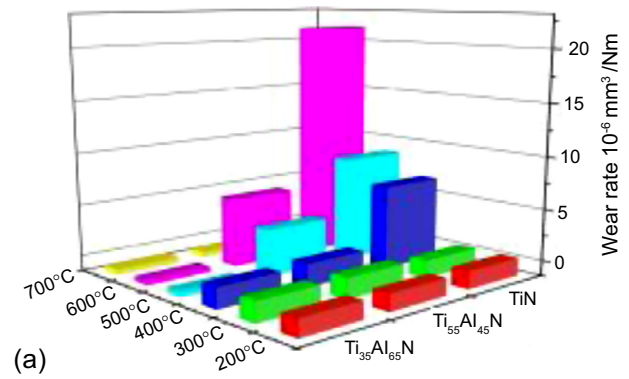
(a)
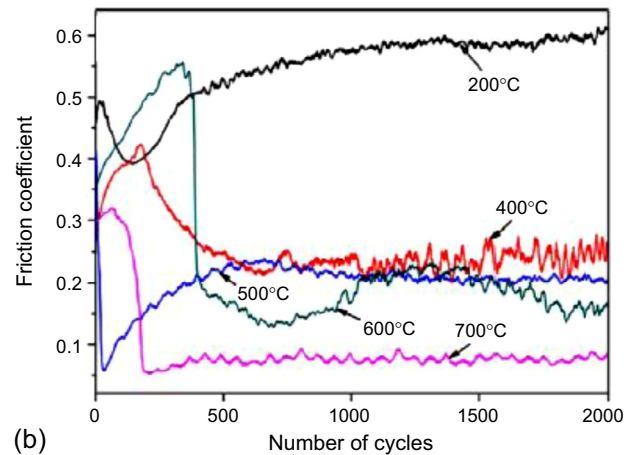
(b)

Figure 6. (a) Wear rates of TiN, $Ti_{55}Al_{45}N$ and $Ti_{35}Al_{65}N$ coatings at different temperatures (from Figure 8 of [52]); (b) Variation of friction coefficient of $Ti_{35}Al_{65}N$ coating with the number of cycles at different temperatures (from Figure 7 of [52]).
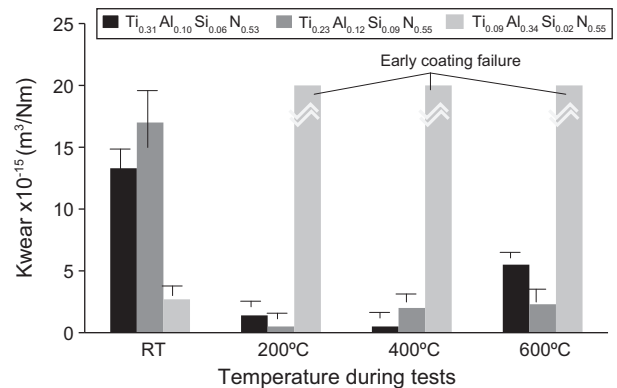

Figure 7. Wear rates of various arc deposited TiAlSiN coatings as a function of the testing temperature (from Figure 4 of [34]).

where the wear rates of these TiAlSiN coatings as a function of the temperature are shown [34]. Clearly, the wear rates of the $Ti_{0.31}Al_{0.1}Si_{0.06}N_{0.53}$, $Ti_{0.23}Al_{0.12}Si_{0.09}N_{0.55}$ coatings at 200 °C, 400 °C and 600 °C are smaller than that measured at RT. The coating with a stoichiometry $Ti_{0.09}Al_{0.34}Si_{0.02}N_{0.55}$ failed at high temperatures probably due to its very high Al content and smaller hardness.
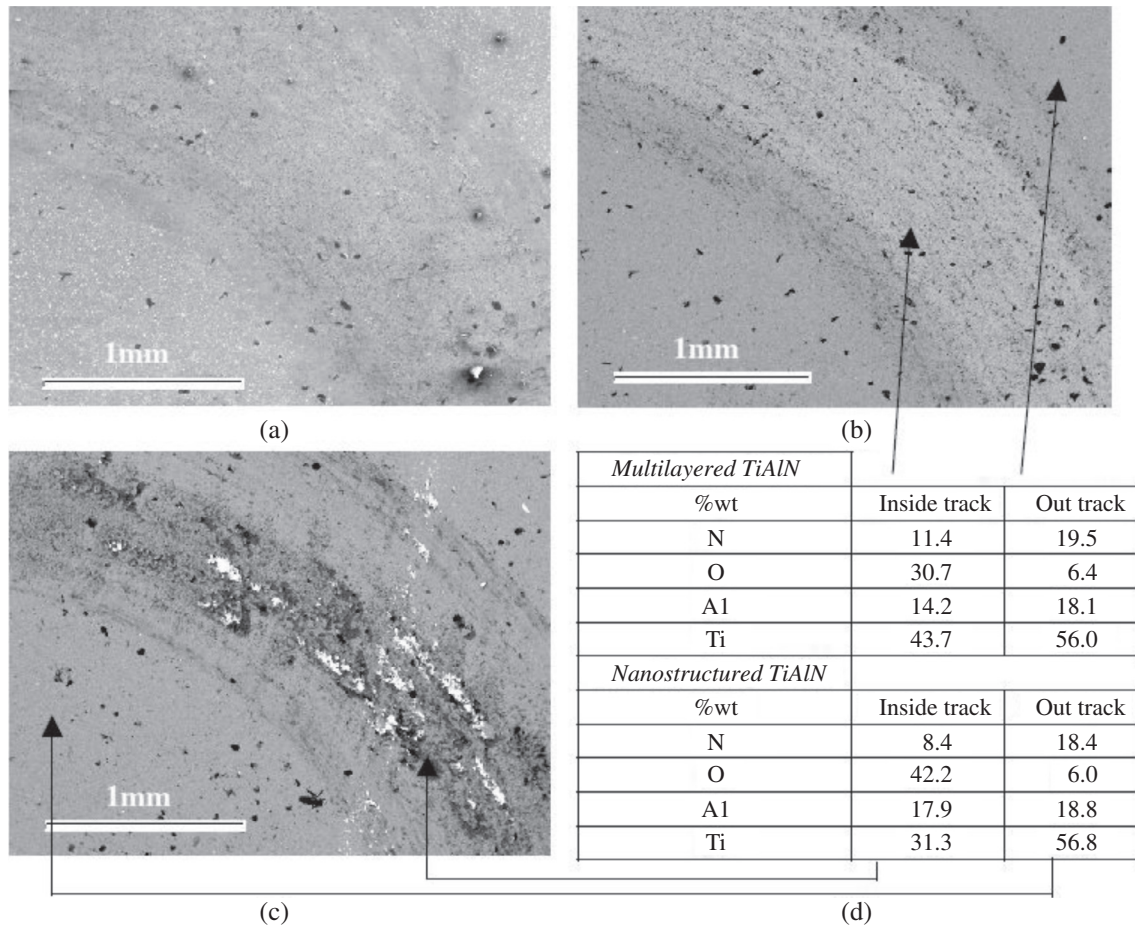
Figure 8. SEM micrograph of samples tested at 500 °C: (a) multilayered coatings (secondary electron mode); (b) multilayered coating (back-scattering mode); (c) nanostructured coating (backscattering mode) and (d) wt% of the multilayered and nanostructured coatings inside and outside the wear scar, respectively (from Figure 5 of [69]).

It is interesting to point out that this behaviour in $Ti_{1-x}Al_xN$ systems was only present for concentrations of Al around $x = 0.6$–0.7, whereas in the TiAlSiN system, this trend is observable for smaller Al concentrations. Staia et al. [69] found a similar behaviour on nanostructured $Ti_{0.6}Al_{0.4}N$ and nanomultilayered $Ti_{0.7}Al_{0.3}N$/TiN deposited on hard metal by cathodic arc evaporation from commercial suppliers; i.e. a reduction of the wear rate as the temperature of the tribological tests were increased to 500 °C. The authors found that the sliding contact areas of these films also developed oxide tribofilms, in agreement to that found in [34], just as shown in Figure 8. The exact nature of the oxide could not be found by means of EDX technique; however, due to the higher affinity of aluminium with oxygen, a layer of Al_xO_y or a mixture of Al_xO_y and Ti_xO_y could have been formed at this temperature according to their thermodynamic behaviour In the case of a single layer $Ti_{0.6}Al_{0.4}N$ coating [69], the increase in testing temperature led to an increase of the wear rate, in agreement with [52, 53], reflecting the importance of the microstructure in the film performances. Qi et al. [70] reported that the wear rate of ion plated $Ti_{0.34}Al_{0.66}N$ decreased progressively when the annealing temperature increased from RT up to 600 °C, increasing the wear rate above this temperature threshold.

3.3. Tribological behaviour at simulation rigs

In order to make a step further in the research of the performance of hard coatings on hot work tools, simulation rigs are frequently utilised before industrial test can be carried out. There are two major reasons; first, conventional lab tribological test systems do not reach contacting conditions (high pressure) as these present in industrial machines or presses; and second, industrial trials are very expensive in terms of tool costs and machine time availability. Simulation test rigs are often self designed systems to meet the industrial conditions targeted, i.e. metal casting, hot forging or extrusion, etc. In addition, and differently to the case of lab tests, vacuum coated tool steels have been previously nitride or carbonitrided in order to provide load support to the hard thin films. Figure 9 depicts two representative high temperature tribology test rigs. Figure 9 (top) represents an inductively heated Al cylinder sliding on a counter H11 tool steel surface. Figure 9 (bottom) represents a cylinder on cylinder set up which includes a heating
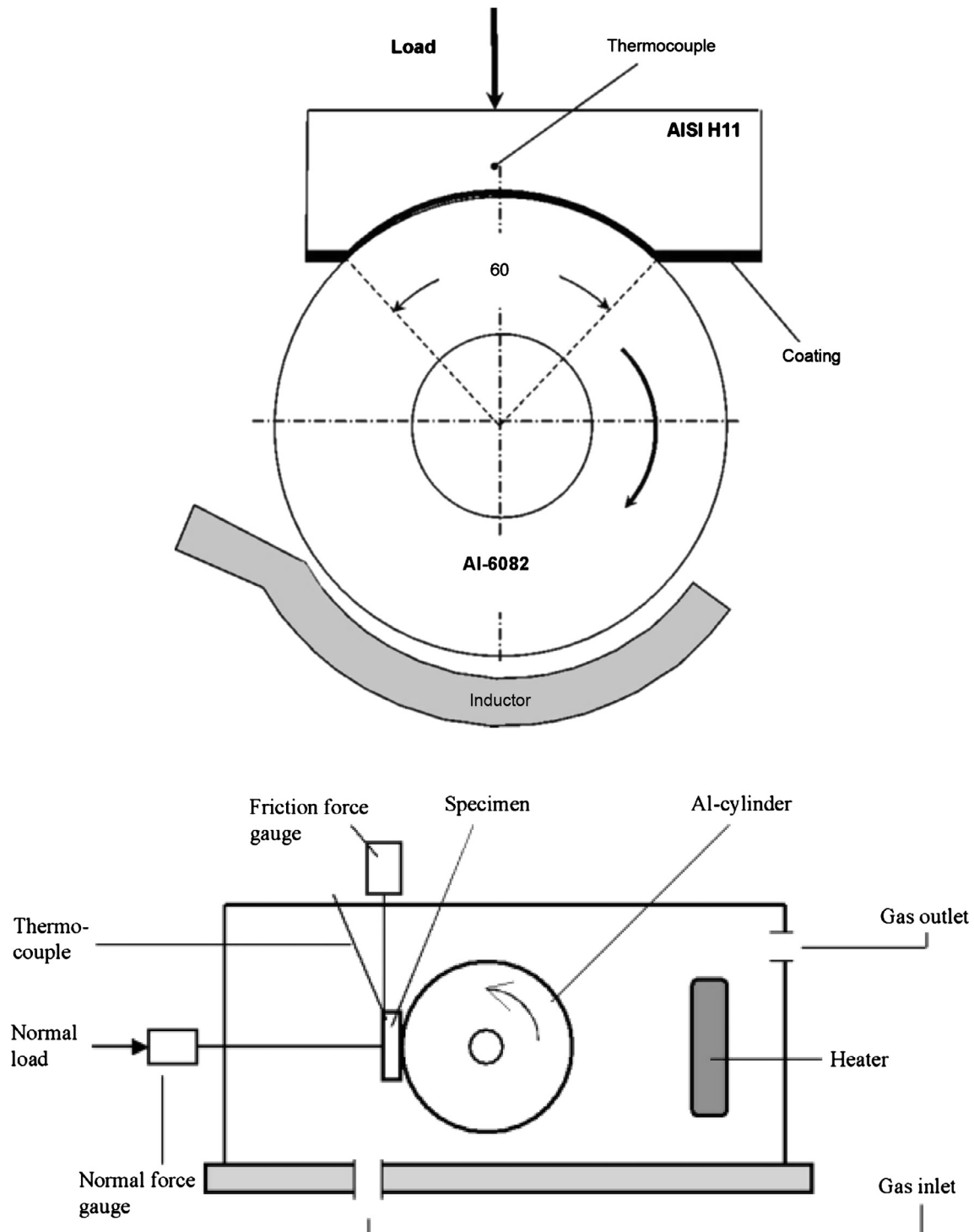
Figure 9. Schemes of some Aluminium hot friction test rig (left, from Figure 1 of [74], and right from Figure 1a of [80]).

unit and load cells for friction force monitoring. Podgornik et al., compared various high temperature test rigs to gain information on the galling properties of contacting surfaces for hot steel sheet forming [71]; pin-on-disc, cylinder-on-cylinder and a new load-scanning test method which involves two crossed cylinders, forced to slide reciprocally against each other under a constant speed. The authors concluded that the load-scanning test method provided a more accurate

assessment of the galling properties between two contacting surfaces, with respect to the cylinder-on-cylinder and the pin-on-disc setups.

The thermal fatigue is also a relevant property in hot forming, for which different test rigs are developed. Smolik et al. [72] applied the so called Coffin's test to characterize the thermal fatigue behaviour of various PVD duplex coating architectures on hot work steel DIN1.2367, and compared
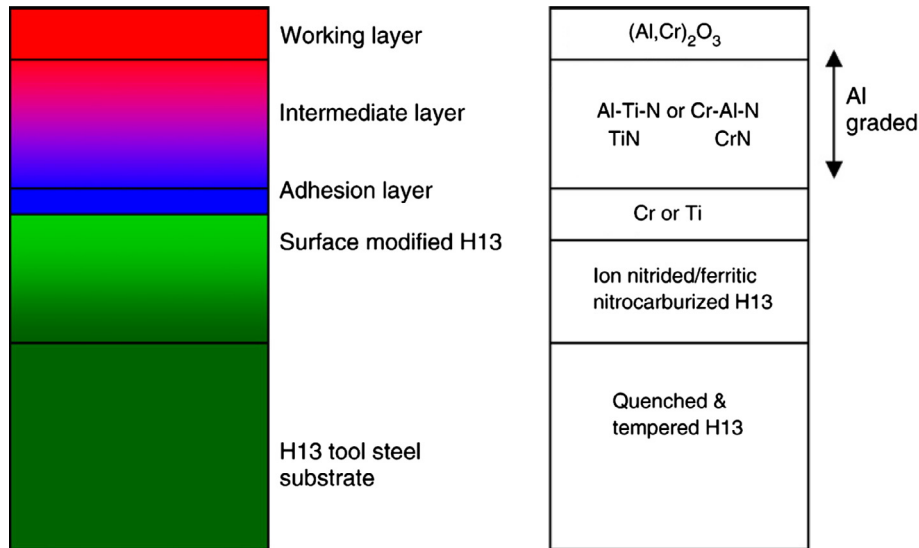
Figure 10. Various multilayered coating designs proposed: (1) Cr$_2$N/graded Cr$_2$N-CrN/Cr/ion nitrided H13, (2) AlTiN/graded Ti-Al-N/TiN/ Ti/ferritic nitrocarburized and (3) TiCB/graded Ti-C-B/Ti/ferritic nitricarburized H13; for a die used in Al pressure die casting (from Figure 13 of [39]).

the results with hot forging operations. The authors found that the thermal fatigue cracking can be reduced by using nitrided PVD support treatments without the compound layer and the precipitation of iron nitrides on the grain boundaries. Persson et al. [40] designed an induction based thermal fatigue tests in combination to strain monitoring in order to investigate the effects of thermal cycling in metal die casting. Srivastava et al. [73] investigated the fatigue resistance, in terms of cracking formation, of PVD multilayered coatings on H13 steels under cycling contact with molten Al. Contrary to previous studies, the authors found that the multilayered structure provided a better response of the H13 surface against cracking formation and propagation.

TiN/CrN multi-layer coating by PVD were reported to provide good impact loading on plasma nitrided H13 steel, and it was proposed as a reliable coating for hot work applications [75]. Klimek et al. [76] studied boron containing hard coatings Ti(B, N) and TiB$_2$ deposited by plasma activated CVD on plasma nitrided Al and Mg die casting and forging tools (X38CrMoV5-1 steel based). Ti(B, N) and TiB$_2$ hard coatings on substrates with the Fe$_2$N$_3$ phase and the mixed phases showed a significant decrease in adhesion compared to Fe$_4$N compound layers or sole diffusion layers. Plasma nitride tool steels and PVD/CVD coatings have been studied for galling prevention at high temperatures [77, 78]. Pelcastre et al. [77] described two different galling initiation mechanisms during the sliding of uncoated and PVD coated tool steels against Al-Si coated high strength steels. Galling initiated through accumulation and compaction of wear debris when untreated tools are used whereas the PVD coatings resulted in increased galling due to adhesion. Birol and Yuksel [79] studied duplex AlTiN coatings on PN AISI H13 hot work tool steel samples under conditions similar to those encountered in hot aluminium extrusion. It was found that Al-based adhesive layer formed on the PN tool steel leading to the fracturing of the diffusion zone upon sliding, followed

by spallation produce a substantial material loss in the nitrided sample. The AlTiN coating, on the other hand, resisted the delamination and protected the underlying steel substrate against a chemical interaction with the aluminium counterface. Björk et al. [80] found that TiB$_2$ coatings exhibited fewer tendencies than TiAlN or CrN coatings to pick up Al during hot extrusion test rigs at 550 °C, although CrN and TiAlN also exhibited good wear resistance. However, TiB$_2$ films were more sensitive than TiAlN to the chemical attack by NaOH during die cleaning. The authors also found that uncoated steel areas worn by removal of continuously formed layers, up to 5 mm thick, of Al-Fe compounds in agreement with [39].

Lin et al. [39] developed a design methodology to identify optimized die coating systems used for a range of material processing dies and specifically applied to aluminium die casting. The methodology is based on determining (i) a working layer that is non wetting with the material being formed, (ii) a graded intermediate layer that can accommodate the residual stresses incurred during the processing/forming cycle, (iii) an adhesion layer, (iv) modification of the surface of the die that interfaces with the optimized coating system. Based on these considerations, the authors proposed in Figure 10 various multilayered coating designs: (1) Cr$_2$N/graded Cr$_2$N-CrN/Cr/ion nitrided H13, (2) AlTiN/graded Ti-Al-N/TiN/Ti/ferritic nitrocarburized and (3) TiCB/graded Ti-C-B/Ti/ferritic nitricarburized H13.

3.4. Novel coating designs

Along with the traditional coating formulations based on transition metal nitrides, novel ternary oxide coatings are attracting the attention of the researchers. In particular the Cr-Al-O system by PVD is gaining the attention of various reputed research groups and companies. The interest on Cr-Al-O responds to the possibility of formulating at temperatures in the range accessible by PVD super hard, thermally stable and oxidation resistance structures exhibiting the corundum

α-Al_2O_3 structure. The reason is that Cr_2O_3 oxides have the same crystallization group R3c than that of α-Al_2O_3, and they can be synthesized at moderate temperatures between 400 and 600 °C by magnetron sputtering and cathodic arc evaporation [81, 82]. Najafi et al. [83] reported on a crystalline phase transition from a cubic structure γ-$(Cr_xAl_{1-x})_2O_3$ to the corundum α-$(Cr_xAl_{1-x})_2O_3$ along a coating thickness of stoichiometry $Al_{0.22}Cr_{0.20}O_{0.57}$ from a 2 microns thick. The performances of these family of coatings have not been tested yet on hot forming applications but only in high speed machining [83], having exhibited good thermal stability and wear resistance. Recent results of our research group suggest that alternating layers of CrAlO/CrAlN deposited by cathodic arc evaporation may result in enhanced wear resistances and better surface quality finishing, which is a requirement for forming tools. Pin on disc tests in the range 200 °C and 500 °C against alumina counterparts are in progress.

3.5. Numerical modelling of thin films performances

In the recent years, the development of predictive numerical tools to anticipate the mechanical performance of coating-substrate systems has gained a notable interest among the tooling protection industrial segment. Accurately predicting the failure of coating-surface systems, including coatings on tools/products, is of significance for all of the parties concerned within the chain of design, manufacturing and use of a product. However, until recently the design and manufacturing of coating/substrate systems still relied largely on the results of experiments and failure tests.

Numerical models, which are able to cope with the effect of all possible parameters of a multi-layered surface system on coating performance, were rarely encountered. In fact, relatively little work had been carried out on the numerical analysis of the failure mechanisms of coatings and substrates.

Previous research has been focused largely on the effect of individual parameters rather than on the performance of a multi-layer system as a whole. The cohesive law introduced [84] enabled coating cracks to be considered physically in analyzing the failure mechanisms of coating/substrate systems. The most recent research investigations, however, did not consider real loading cases rather than focus on indentation or tension tests alone. Further, applications of cohesive-zone modelling only considered single loading conditions, and hence, they are unable to deal with multiple-loading cases such as forming.

New numerical procedures which combines parameterised FE modelling, cohesive-zone modelling, fatigue modelling and a sub-modelling technique has been developed recently [85] to study the initiation and propagation of plastic deformation in the substrate material of a coated tool-steel (TiN coating on Nitrided 42CrMo4) and their effect on the failure of the coating due to fracture [86, 87]. It has also been used to predict the critical loading on tools [87].

Numerical modelling algorithms accounting with the effects of temperature, friction or material adhesion are still a challenge to be developed at scientific and industrial level.

4. Field trials of thin films in hot working applications

In general, industrial field validation tests are scarcely present in the scientific literature probably due to their high costs of realization. Despite of this, there are some interesting field trial studies worthy to be discussed here. Sokovic et al. [88] studied the effect of CrN PVD coating + PN duplex treatment onto H11 die-casting dies for the fabrication of driving wheels. Their results suggested that duplex treatment improved the wear rate of some specific die parts over the performance exhibited by the untreated and the PN dies. In contrast, the die gate surface could not be efficiently protected due to the extreme conditions given by the pressure and sliding speed of the molten Al at this site. Various failure mechanisms were identified such as coating oxidation, aluminium welding and fracture propagation from the surface to the core.

Panjan et al. [89] studied the performance of AISI H11 hot work steel, untreated, plasma nitrided and Duplex PVD coated + plasma nitrided, during forging of DIN ST52-3 construction steel preheated at 1050 °C. The authors found that the Duplex treated steels outperformed these untreated and plasma nitrided. In fact, they observed that the TiAlN/TiN PVD multilayer remained intact at the short sliding length parts of the die, only exhibiting partial delamination at the largest sliding length parts.

Müller [90] carried out industrial tests in hot extrusion product lines on AA6061 aluminium alloys at a billet temperature of 495 °C. The authors characterized the extruded surface roughness as an indirect indicator of the tool surface quality, being the critical value for tool replacement of Rz higher 25 mm. They concluded that duplex treated consisting of PACVD TiBN + PN outperformed by a factor six over untreated X38CrMoV5-1 steel dies.

Navinsek et al. [91] studied the applications of CrN, PN-CrN and PN-TiAlN in aluminium pressure die-casting, CrN in hot extrusion of Al and TiN/TiAlN and PN- TiN/TiAlN coating in hot forging of steel parts, as shown in Figure 11. The results reported showed important improvement in tool or die life cost saving. More important than pure tool saving costs, it was mostly appreciated the better reproducibility of the surface quality of the products obtained, an increase in the manufacturing reliability in heavy machining, and a decrease in production down-time.

Pellizzari et al. [92] identified the occurrence of two distinct damage regimes in aluminium hot extrusion at 350 °C. Regime 1 showed minor variations of the COF. Regime 2 was characterized by fully plastic Al-Al contact, with large fluctuations of the COF. The authors defined as the transition time as indicative of the ability of a surface layer in delaying the occurrence of regime 2. This time is correlated to the chemical compatibility of the surface layer (compound layer, PVD or CVD coating) versus Al. Severe form of wear was observed by nitrided steels while a localised and less severe form of wear was present on duplex treated, nitriding + PVD steel. No wear traces were observed by CVD TiC + TiN coated steel, providing this latter the best performance among the surface treatments investigated. Mitterer et al. [93] studied the deposition of TiN based coatings on Al die-casting dies by
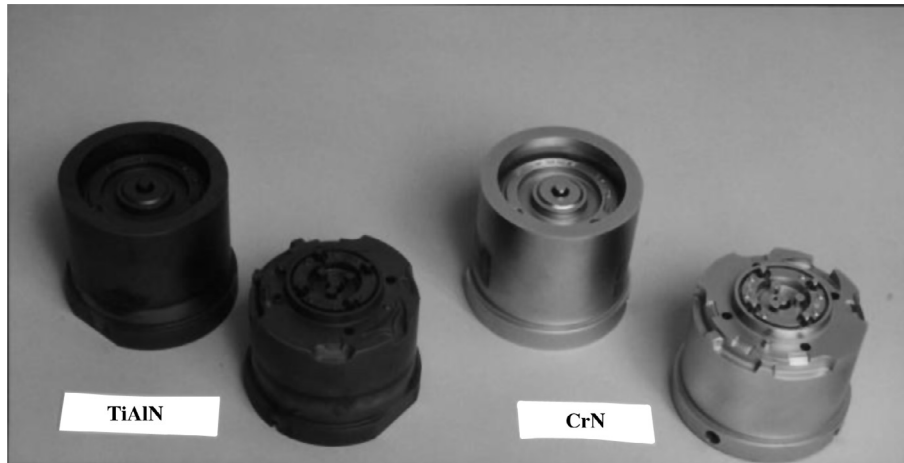
Figure 11. Pressure die casting of Al12Si alloy with cores and dies, improved with TiAlN and CrN coating (from Figure 1 of [91]).

Figure 12. Two die parts (left) an untreated and (right) a duplex treated with an arc evaporated TiAlSiN coating on top of a plasma nitrided AISI H13 die, after 50,000 Al-injection shots done in a manufacturing plant.

magnetron sputtering and PACVD. They reported on improvements of several hundred percents of the deposited dies with respect to the non-deposited elements.

The efficiency of duplex treated Al die-casting dies is under investigation in our lab at Center of Advanced Surface Engineering of AIN. Figure 12 shows two die parts (left) an untreated and (right) a duplex treated with an arc evaporated TiAlSiN coating on top of a plasma nitrided AISI H13 die, after 50,000 Al-injection shots done in a manufacturing plant. The untreated die cavity after 50,000 shots exhibits accumulation of soldered aluminium on various sectors (see red lines). In contrast, the duplex treated die cavity does not show any hint of Al galling or thermal fatigue. Even more, TiAlSiN PVD coatings have also been tested on AISI H13 die inserts, typically used as work piece ejector, and compared to TiAlN coatings. Figure 13 shows the pictures of (left) TiAlN and (right) TiAlSiN coated PN H13 inserts after 100 k Al-injection shots

have been carried out in an industrial Al die casting press. The surfaces of the TiAlN coated inserts show evidence of thermal fatigue effect in the form of shine loses and presence of small surface defects, due to different attack mechanisms of crack initiation and propagation and chemical attack of aluminium on the naked steel metal. In contrast, the TiAlSiN coated insert surfaces retain the surface quality even after this amount of injection cycles.

It is interesting to highlight the existing correlation between the tribological tests on TiAlN and TiAlSiN coatings with the results of this industrial validation. The tribological response of TiAlN coatings at high temperatures was characterized by a reduction of the COF but also an increase of the wear rate with respect to that at RT due probable to the combination of various factors such as crack initiation by thermal fatigue. TiAlSiN coatings, on the other hand, showed a remarkable wear rate reduction at temperature between 200 and
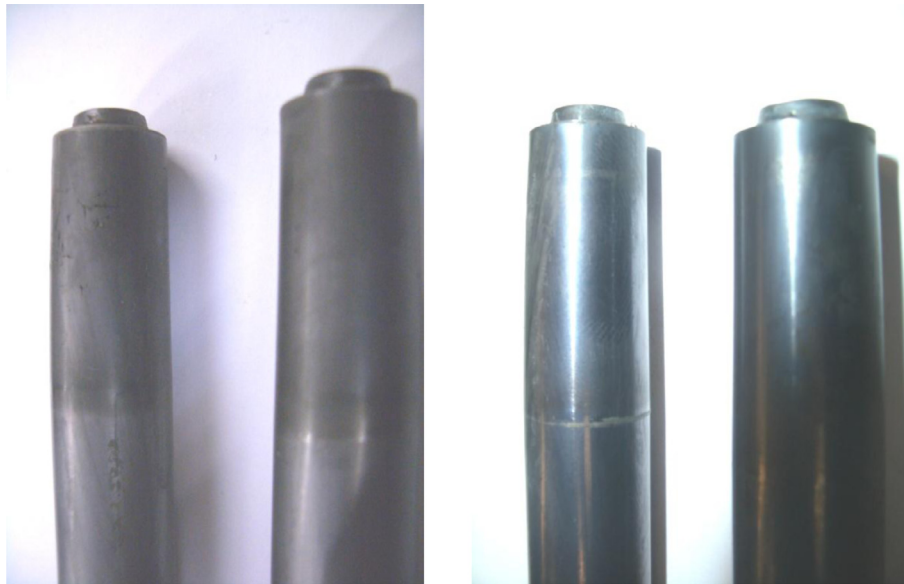
Figure 13. (left) TiAlN and (right) TiAlSiN coated PN H13 inserts after 100 k Al-injection shots have been carried out in an industrial Al die casting press.

600 °C due to the formation of a tribofilm on the areas of sliding contact. Also, the grain refinement induced by Si can be responsible for the reduction of thermal fatigue processes.

5. Discussion and final remarks

Hot work tooling protection by vapour deposited coatings is not only an interesting scientific topic but also an economically impacting challenge driven by an urgent industrial demand. Physical and chemical vapour deposition technologies are at the front edge of the current research tendencies in hot work tooling protection, and various successful examples (at least at lab scale) can be found. In this scenario, the analysis of the reported studies seem addressing a restricted number of coating formulations, which are valid for aggressive working conditions such as high temperature, load contact stresses, abrasive and adhesive wear and thermal shocking. Thus, the system Ti-Al-N with the occasional incorporation of impurities such as Si, or C, either in the form of a single solid solution phase or forming more complex micro or nano scaled structures, is one of the most highly performing coating systems for hot forming tools. However, open questions regarding the influence of the coating stoichiometry and microstructure on the wear behaviour at medium-high temperature still remain. For example, from the analysis of the literatures available, it has been found that for Al concentrations in the $Ti_{1-x}Al_xN$ system below 0.6, these coatings exhibits a progressive increase of their wear rates when the temperature of the tests is increased from RT to the 600–700 °C. However, for Al contents in the range $0.6 < x < 0.7$, where the formation of less hard wurtzite type h-AlN phases is not yet promoted, the coatings show the opposite wear behaviour; that is to say, a reduction of the wear rate as the testing temperatures increase. It has been also found that the addition of Si can also

promote this "*anomalous*" behaviour in these coating systems with even smaller amounts of Al. Differences in the chemical nature of the formed tribo-films, the changes in the local microstructure when the stoichiometries are near to the transition thresholds between stable solid solution phases and multi-phase segregation could be behind this observed behaviours. A thorough investigation of the influence of the stoichiometry of the TiAlN in the temperature driven tribology is proposed, not only due to scientific reasons but also because it may have an enormous industrial impact.

Another coating formulation system receiving intensive research efforts is the Cr-Al-N, and as in the case of Ti-Al-N, their combinations with allying elements such as Si or heavier elements like Hf, or Y. All the literature coincides to the fact that these coating formulations exhibit a high thermal stability and an outstanding oxidation resistance, even at temperatures exceeding 900–1000 °C. In addition, these coatings show excellent wear resistance at RT. However these coatings seem not to perform optimally or they even fail when the tribological tests are carried out in the range of 400–700 °C (note that numerous hot forming applications take place in this T range). Comprehensive studies providing satisfactory scientific explanations on this thermal-tribological behaviour are not present in the literature so far. One hypothesis of the relative low wear performance of these films at medium-high temperatures is that the oxide scales formed at the sliding contact zones are extremely thin and mechanically weaker than these formed on TiAlN coatings. This issue is under research in our laboratory. The formation of stable fcc-CrAlNO or super-hard corundum like $(Cr, Al)_2O_3$ phases seem alternatives to develop highly performing Cr-Al based coatings for hot work applications (see Sect. 3.4 for more details on these coatings). The system TiB_2 and TiBN or their compositing in the form of TiN/BN have also received an important attention for hot work applications due to the low adhesive properties of the TiB_2 at

medium temperatures. However, its low resistance to oxidation, due to the low melting point of boron oxide (450 °C), and its relatively chemical unstability against alkaline washing fluids restrict its application in hot work tools.

Current trends in vapour deposited coatings does not restrict to only intrinsically superhard materials, but more importantly on the search of specific nanostructures combining high hardness, toughness, thermal fatigue and oxidation resistance. Veprek [1] argues that the first approach is not of practical use in industry as the intrinsically hard materials are not fully stable. Contrarily, the search of novel metastable multi-materials with decreasing crystalline domains in the nanometer scale (10–15 nm), and therefore an increasing dislocation blocking sites should focus the research endeavours. Stueber et al. [31] coincides in this analysis and proposes intensive research efforts in the study of multiphase nanocomposite materials, combining for example amorphous and polycrystalline hard phases [31, 94, 95]; and alternatively hard metastable materials with coherent local order [45, 46, 94–96].

However, all of these research current trends need to be made fully compatible with coating industrial systems of job coating centres, if a real industrial impact is to be attained. For example, the Veprek approach on nanocomposites is limited by the fact that in order to realize the maximal potential of these coating formulations oxygen percentage should be smaller than 100 ppm, which is difficult to attain for large industrial coating systems. Also, the industrial development of coatings containing lubricious elements such as V might have difficulties due to the toxicity of potentially formed by-products such as vanadium oxides.

With regards to the implantation of vapour deposited coatings on the hot work industry, as briefly introduced in Section 4, experimental costs are the largest barrier for industrial validation and acceptance. Cost of moulds or dies may range from 10 to 100 k€. If various coatings wish to be tested and with a robust statistical relevance, the total costs become unaffordable for most academic groups or for SMEs involved in coating research. The availability of manufacturing plants and the time needed to carry out inspection and analysis represent additional costs. This, given the narrow margins of the EU manufacturing industry, makes most SMEs unable to perform fully reliable validation tests. All these make of very high relevance the realization of adequate tribological analysis, in standard lab equipment and later in specific purpose made test rigs.

In conclusion, this work has provided with a concise but industrially focused view over the present vapour coatings for the hot work tooling sector. As having been shown, the scientific and technical literatures offer a great amount of information on the lab-scale temperature-dependent coating system performance and less amount on the full field-trials studies, mostly, due to the high costs involved. Current research has been focused significantly on the nanostructuring of well-known metastable hard phases, which, in combination, can provide excellent properties suitable for hot work environment. All together, along with the strengthening of the industry and academia cooperation and with the support of public-private funds (specially support to the realization of more reliable validation tests), will help to realize full potential of vapour coatings for this important manufacturing sector.

References

1. S. Veprek, Journal of Vacuum Science & Technology A 17 (1999) 2401–2420 and J. Vac. Sci. Technol. A **31** (2013) 050822-1.
2. K. Holmberg, A. Mathews, in: Coatings Tribology, 2nd edition by B.J. Briscoe, Elsevier.
3. K. Bobzin, N. Bagcivan, A. Reinholdt, M. Ewering, Surface and Coatings Technology 205 (2010) 1444–1448.
4. G.S. Fox-Rabinovich, A.I. Kovalev, J.L. Endrino, S.C. Veldhuis, L.S. Shuster, I.S. Gershman, in: G.S. Fox-Rabinovich, G. Totten (Eds.), Chapter 9 Surface-Engineered Tool Materials for High-Performance Machining, Taylor and Francis Books/ CRC Press LLC, USA, 2007.
5. G.S. Fox-Rabinovich, J.L. Endrino, B.D. Beake, A.I. Kovalev, S.C. Veldhuis, L. Ning, F. Fontaine, A. Gray, Surface and Coatings Technology 201 (2006) 3524–3529.
6. L. Hultman, Vacuum 57 (2000) 1–30.
7. G.G. Fuentes, D. Caceres, I. Vergara, E. Elizalde, J.M. Sanz, Surface and Coatings Technology 151–152 (2002) 365.
8. S.J. Bull, D.G. Bhat, M.H. Staia, Surface and Coatings Technology 163–164 (2003) 507–514.
9. S. PalDey, S.C. Deevi, Material Science and Engineering A 342 (2003) 58–79.
10. G.G. Fuentes, R. Rodriguez, J.C. Avelar-Batista, J. Housden, F. Montalá, L.J. Carreras, A.B. Cristóbal, J.J. Damborenea, T.J. Tate, Journal of Materials Processing Technology 167 (2005) 415.
11. T. Polcar, R. Martinez, T. Vítů, L. Kopecký, R. Rodriguez, A. Cavaleiro, Surface and Coatings Technology 203 (2009) 3254–3259.
12. G.G. Fuentes, M.J. Diaz de Cerio, A. García, R. Martínez, R. Bueno, R.J. Rodríguez, M. Rico, F. Montalá, Yi. Qin, Surface and Coatings Technology 203 (2008) 670–674.
13. W. Kalss, A. Reiter, V. Derflinger, C. Gey, J.L. Endrino, International Journal of Refractory Metals and Hard Materials 24 (2006) 399–404.
14. R.J. Rodríguez, J.A. García, R. Martínez, B. Lerga, M. Rico, G.G. Fuentes, A. Guette, C. Labruguere, M. Lahaye, Applied Surface Science 235 (2004) 53–59.
15. S. Carrera, O. Salas, J.J. Moore, Surface and Coatings Technology 167 (2003) 25–32.
16. Rointan F. Bunshah (Ed.), Handbook of hard coatings, Deposition Technologies, Properties and Applications, William Andrew Publishing, LCC, 2001, ISBN: 0-8155-1438-7.
17. J. Musil, H. Hrubý, Thin Solid Films 365 (2000) 104–109.
18. A. Hörling, L. Hultman, M. Odén, J. Sjölén, L. Karlsson, Journal of Vacuum Science & Technology A20 (2002) 1815–1823.
19. Z. Ding, C.T. Bui, X.T. Zeng, Surface and Coatings Technology 203 (2008) 680–684.

20. E. Ribeiro, L. Rebouta, S. Carvalho, F. Vaz, G.G. Fuentes, R. Rodriguez, M. Zazpe, E. Alves, Ph. Goudeau, J.P. Riviere, Surface and Coatings Technology 188–189 (2004) 351.

21. H. Scheerer, T.H. Hoche, E. Broszeit, B. Schramm, E. Abele, C. Berger, Surface and Coatings Technology 200 (2005) 203–207.

22. J.L. Endrino, V. Derflinger, Surface and Coatings Technology 200 (2005) 988–992.

23. S.-Y. Lee, Yeh-Sun Hong, Surface and Coatings Technology 202 (2007) 1129–1134.

24. M.G. Faga, G. Gautier, R. Calzavarini, M. Perucca, E. Aimo Boot, F. Cartasegna, L. Settineri, Wear 263 (2007) 1306–1314.

25. S.K. Kim, P.V. Vinh, J.H. Kim, T. Ngoc, Surface and Coatings Technology 200 (2005) 1391–1394.

26. A. Flink, J.M. Andersson, B. Alling, R. Daniel, J. Sjölén, L. Karlsson, L. Hultman, Thin Solid Films 517 (2008) 714–721.

27. J.L. Endrino, S. Palacín, M.H. Aguirre, A. Gutiérrez, F. Schäfers, Acta Materialia 55 (2007) 2129–2135.

28. D. Rafaja, M. Dopita, M. Růžička, V. Klemm, D. Heger, G. Schreiber, M. Šíma, Surface and Coatings Technology 201 (2006) 2835–2843.

29. A.A. Voevodin, S.D. Walck, J.S. Zabinski, Wear 203 (1997) 516–527.

30. K. Holmberg, A. Matthews, H. Ronkainen, Tribology International 31 (1998) 107–120.

31. M. Stueber, H. Holleck, H. Leiste, K. Seemann, S. Ulrich, C. Ziebert, Journal of Alloys and Compounds 483 (2009) 321–333.

32. M. Diserens, J. Patsheider, F. Lévy, Surface and Coatings Technology 108–109 (1998) 241–246.

33. F. Vaz, L. Rebouta, S. Ramos, M.F. da Silva, J.C. Soares, Surface and Coatings Technology 108–109 (1998) 236–240.

34. G.G. Fuentes, E. Almandoz, R. Pierrugues, R. Martínez, R.J. Rodríguez, J. Caro, M. Vilaseca, Surface and Coatings Technology 205 (2010) 1368–1373.

35. J. Böhlmark, Fundamentals of High Power Impulse Magnetron Sputtering, Dissertation No. 1014, Linköping Institute of Technology, Sweden.

36. J. Chen, X.Y. Li, R. Ji, R. Khan, G. Fuentes, Surface Engineering 29 (2013) 462–467.

37. R. Hoya, J.-D. Kammingaa, G.C.A.M. Janssen, Surface and Coatings Technology 200 (2006) 3856–3860.

38. J.C. Avelar-Batista, E. Spain, G.G. Fuentes, A. Sola, R. Rodriguez, J. Housden, Surface and Coatings Technology 201 (2006) 4335–4340.

39. J. Lin, S. Carrera, A.O. Kunrath, D. Zhong, S. Myers, B. Mishra, P. Ried, J.J. Moore, Surface and Coatings Technology 201 (2006) 2930–2941.

40. A. Persson, S. Hogmark, J. Bergström, Surface and Coatings Technology 191 (2005) 216–227.

41. X. Ma, K. Yukimura, Surface and Coatings Technology 186 (2004) 88–92.

42. G.G. Fuentes, P. Prieto, C. Morant, C. Quirós, R. Núñez, E. Elizalde, J.M. Sanz, Physical Review B 63 (2001) 075403.

43. G.G. Fuentes, E. Elizalde, J.M. Sanz, Journal of Applied Physics 90 (2001) 2737.

44. P.H. Mayrhofer, C. Mitterer, L. Hultman, H. Clemens, Progress in Materials Science 51 (2006) 1032–1114.

45. P.H. Mayrhofer, C. Mitterer, H. Clemens, Advanced Engineering Materials 7 (2005) 1071–1082.

46. P.H. Mayrhofer, F.D. Fischer, H.J. Böhm, C. Mitterer, J.M. Schneider, Acta Materialia 55 (2007) 1441–1446.

47. X.-Z. Ding, X.T. Zeng, Y.C. Liu, Thin Solid Films 519 (2011) 1894–1900.

48. S. Zhang, L. Wang, Q. Wang, M. Li, Surface and Coatings Technology 214 (2013) 160–167.

49. Y.-Y. Chang, C.-P. Chang, D.-Y. Wang, S.-M. Yang, W. Wu, Journal of Alloys and Compounds 461 (2008) 336–341.

50. S.B. Won, M.J. Kim, C.Y. Xu, Y.S. Hwang, D.B. Lee, Advanced Materials Research 69 (2013) 612–615.

51. J. Martan, P. Benes, Thermochimica Acta 539 (2012) 51–55.

52. D. Jianxin, L. Aihua, International Journal of Refractory Metals and Hard Materials 41 (2013) 241–249.

53. K. Kutschej, P.H. Mayrhofer, M. Kathrein, P. Polcik, R. Tessadri, C. Mitterer, Surface and Coatings Technology 200 (2005) 2358–2365.

54. K. Kutschej, T.N. Fateh, P.H. Mayrhofer, M. Kathrein, P. Polcik, C. Mitterer, Surface and Coatings Technology 200 (2005) 113–117.

55. J.C. Walker, I.M. Ross, C. Reinhard, W.M. Rainforth, P.Eh. Hovsepian, Wear 267 (2009) 965–975.

56. P.Eh. Hovsepian, D.B. Lewis, Q. Luo, W.-D. Münza, P.H. Mayrhofer, C. Mitterer, Z. Zhou, W.M. Rainforth, Thin Solid Films 485 (2005) 160–168.

57. T. Polcar, T. Vitu, J. Sondor, A. Cavaleiro, Plasma Processes and Polymers 6 (2009) S935–S940.

58. T. Polcar, A. Cavaleiro, Surface and Coatings Technology 206 (2011) 1244–1251.

59. Z. Zhou, W.M. Rainforth, Q. Luo, P.Eh. Hovsepian, J.J. Ojeda, M.E. Romero-Gonzalez, Acta Materialia 58 (2010) 2912–2925.

60. S.M. Aouadi, D.P. Singh, D.S. Stone, K. Polychronopoulou, F. Nahif, C. Rebholz, C. Muratore, A.A. Voevodin, Acta Materialia 58 (2010) 5326–5331.

61. N. Fateh, G.A. Fontalvo, G. Gassner, C. Mitterer, Wear 262 (2007) 1152–1158.

62. R. Franz, C. Mitterer, Surface and Coatings Technology 228 (2013) 1–13.

63. K. Kutschej, P.H. Mayrhofer, M. Kathrein, P. Polcik, C. Mitterer, Surface and Coatings Technology 188–189 (2004) 358–363.

64. K. Bobzin, N. Bagcivan, M. Ewering, R.H. Brugnara, S. Theiß, Surface and Coatings Technology 205 (2011) 2887–2892.

65. C. Muratore, J.J. Hu, A.A. Voevodin, Thin Solid Films 515 (2007) 3638–3643.

66. D.S. Stone, S. Harbin, H. Mohseni, J.-E. Mogonye, T.W. Scharf, C. Muratore, A.A. Voevodin, A. Martini, S.M. Aouadi, Surface and Coatings Technology 217 (2013) 140–146.

67. J. Hardell, B. Prakash, International Journal of Refractory Metals and Hard Materials 28 (2010) 106–114.

68. J.C. Sánchez-López, A. Contreras, S. Domínguez-Meister, A. García-Luis, M. Brizuela, Thin Solid Films 550 (2014) 413–420.

69. M.H. Staia, M. D'Alessandria, D.T. Quinto, F. Roudet, M. Marsal Astort, Journal of Physics Condensed Matter 18 (2006) S1727–S1736.

70. Z.B. Qi, P. Sun, F.P. Zhu, Z.T. Wu, B. Liu, Z.C. Wang, D.L. Peng, C.H. Wu, Surface and Coatings Technology 231 (2013) 267–272.

71. B. Podgornik, S. Hogmark, J. Pezdirnik, Wear 257 (2004) 843–851.

72. J. Smolik, M. Gulde, J. Walkowicz, J. Suchanek, Surface and Coatings Technology 180–181 (2004) 506–511.

73. A. Srivastava, V. Joshi, R. Shivpuri, R. Bhattacharya, S. Dixit, Surface and Coatings Technology 163–164 (2003) 631–636.

74. M. Pellizzari, Wear 271 (2011) 2089–2099.

75. S. Yul Lee, Surface and Coatings Technology 193 (2005) 55–59.

76. K.S. Klimek, H. Ahn, I. Seebach, M. Wang, K.-T. Rie, Surface and Coatings Technology 174–175 (2003) 677–680.

77. L. Pelcastre, J. Hardell, B. Prakash, Tribology International 67 (2013) 263–271.

78. E. Konca, Y.-T. Cheng, A.M. Weiner, J.M. Dasch, A. Erdemir, A.T. Alpas, Surface and Coatings Technology 200 (2005) 2260–2270.

79. Y. Birol, B. Yuksel, Surface and Coatings Technology 207 (2012) 461–466.

80. T. Björk, M. Berger, R. Westergard, S. Hogmark, J. Bergström, Surface and Coatings Technology 146–147 (2001) 33–41.

81. M. Witthaut, R. Cremer, K. Reichert, D. Neuschütz, Microchimica Acta 133 (2000) 191.

82. J. Ramm, M. Ante, T. Bachmann, B. Widrig, H. Brändle, M. Döbeli, Surface and Coatings Technology 202 (2007) 876–883.

83. H. Najafi, A. Karimi, P. Dessarzin, M. Morstein, Surface and Coatings Technology 214 (2013) 46–52.

84. X.P. Xiu, A. Needleman, Journal of Mechanics and Physics of Solid 42 (1994) 1397–1434.

85. J. Feng, Y. Qin, Q. Zeng, E. Almandoz, G. Fuentes, R.R. Koodakal, J. Michler, Journal of Multiscale Modelling 3 (2011) 1–22.

86. J. Feng, Y. Qin, R.R. Koodakal, J. Michler, Submitted to the Proceedings of the Institution of Mechanical Engineers Part B: Journal of Engineering Manufacture (2012) accepted for publication.

87. D. Yin, X. Peng, Y. Qin, Z. Wang, Journal of Multiscale Modelling 3 (2011) 65–78.

88. M. Sokovic, P. Panjan, M. Cekada, International Journal of Microstructure and Materials Properties 1 (2006) 231.

89. P. Panjan, I. Urankar, B. Navinsek, M. Tercelj, R. Turk, M. Cekada, V. Leskovsek, Surface and Coatings Technology 151–152 (2002) 505–509.

90. K.B. Müller, Journal of Materials Processing Technology 130–131 (2002) 432–437.

91. B. Navinsek, P. Panjan, I. Urankar, P. Cvahte, F. Gorenjak, Surface and Coatings Technology 142–144 (2001) 1148–1154.

92. M. Pellizzari, M. Zadra, A. Molinari, Surface Engineering 23 (2007) 165–168.

93. C. Mitterer, F. Holler, F. Üstel, D. Heim, Surface and Coatings Technology 125 (2000) 233–239.

94. H. Holleck, Surface and Coatings Technology 36 (1988) 151–159.

95. M. Stüber, U. Alberts, H. Leiste, S. Ulrigh, H. Holleck, P.B. Barna, A. Kovacs, P.Eh. Hovsepian, I. Gee, Surface and Coatings Technology 200 (2006) 6162–6171.

96. C. Ziebert, U. Albers, M. Stüber, S. Ulrich, Plasma Processes and Polymers 6 (2009) S560–S565.